表5　心筋症外症例に対する補助人工心臓の適応
(1980—2004/8)
適応理由別臨床成績

	症例(%)	離脱(%)	生存(%)[1]	(%)[2]
ECC離脱困難	229 (55.6)	103 (45.0)	59 (25.8)	(57.3)
術後 LOS#	116 (28.2)	40 (34.5)	26 (22.4)	(65.0)
心原性循環不全##	67 (16.3)	24 (35.8)	19 (28.4)	(79.2)
計	412 (100.0)	167 (40.5)	104 (25.2)	(62.3)

1)：生存症例／適応症例，2)：生存症例／離脱症例　(不明例除く)
#：施行中3例および移植1例を含む
##：施行中4例，移植2例および他システムへの移行1例を含む
(BVS-5000症例を除く)　(日本臨床補助人工心臓研究会)

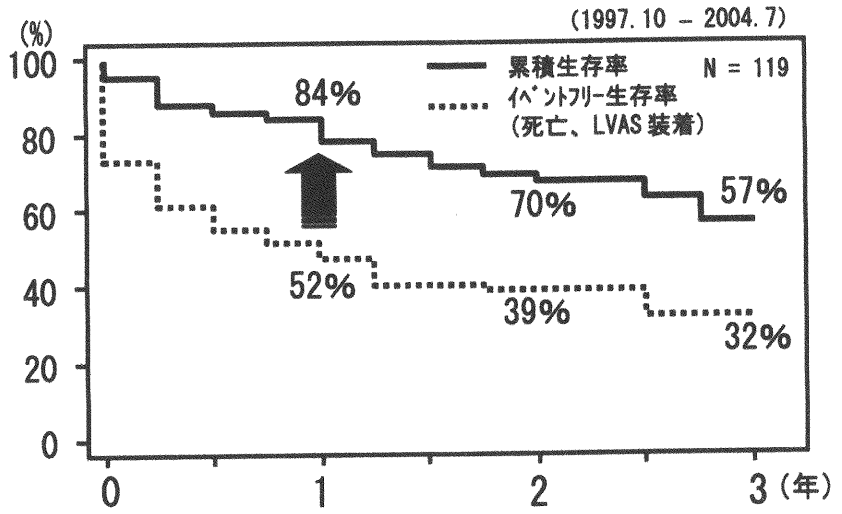

図4　心臓移植適応患者のイベントフリー生存率
(1997年10月から2004年7月までの検討例)

トを行う。

わが国での臨床成績

日本臨床補助人工心臓研究会レジストリー2004年の報告(1980—2004.8)では，わが国でこれまでに補助人工心臓が697例に適応されている。心筋症以外の急性心不全症例では表5に示すように412例に適応されており，41%が離脱し，25%が生存している。また，BVS-5000適応例は61例で，43%が離脱し，28%が生存している。

心筋症に対しては1992年から適用されるようになり，これまでに219例に施行されている。システムは東洋紡製左室脱血型が98例で，他に東洋紡左房脱血型63例，ゼオン製15例，Novacor LVAS 19例，HeartMate-IP 17例，HeartMate-VE 7例であった。補助日数は平均228日，最長1245日で，33例が1年以上の補助であった。また，東洋紡左室脱血型は平均303日，最長1245日であった。移植へ至った症例は28例(国内15例，渡航13例)あり，心機能の改善を34例に認め離脱している。

わが国での心臓移植例は2005年3月までに27例であるが，その内19例はLVAS施行例であった。その補助日数は平均623日，最長1227日(東洋紡製左室脱血型)で，13例が1年以上の補

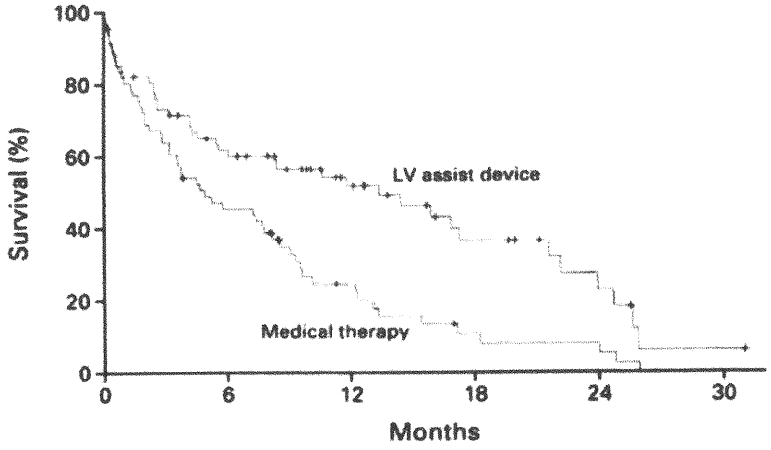

No at Risk						
LV assist device	68	38	22	11	5	1
Medical therapy	61	27	11	4	3	0

図5 REMATCH study における左心補助人工心臓装置例と内科的治療における累積生存率[4]

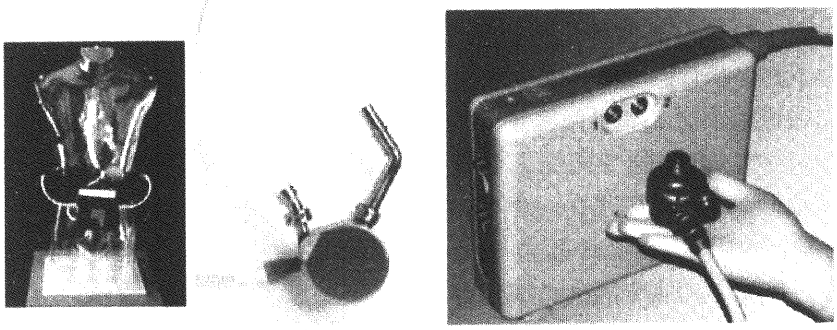

図6 わが国で開発された遠心ポンプによる体内植込み型左心補助人工心臓
左：SunMedical 社製 EvaHeart
右：Terumo 社製 DuraHeart

助例であった。用いられたシステムは，東洋紡製13例，Novacor LVAS 2例，HeartMate-IP 2例，HeartMate-VE 2例であった。

当施設における慢性心不全急性増悪例に対するLVAS適応例は67例であるが，その補助期間は平均411日，最長1245日であった。19例は平均523日の補助後心臓移植（国内11例，渡航8例）され，8例が平均149日後に離脱し，10例が施行中で，30例が平均395日の補助後死亡した。なお，離脱例では，計画的に離脱した7例は全例生存し最長10年を越えている。また，当施設で心臓移植適応ありと判定した患者119例における1年および3年累積生存率は，各々84%および57%と良好であるが，LVAS装着および死亡のイベントフリー生存率は各々52%および32%であり，生存率のLVASによる著明な改善を認めた（図4）。

今後の展望

重症心不全症例において，各種治療法の限界を超えた場合にはVASによる長期補助による心機能の回復あるいは心臓移植へのブリッジについて考慮すべきである。近年心臓移植の適応とされる重症心不全例におけるVASによる自己心機能改善・離脱例が注目され，成長ホルモン療法や細胞移植など離脱の可能性を高める併用手段の研究が

積極的に行われるようになった。また，最近では，VASによるdestination therapyへの関心が高まり，心臓移植非対象例に対する体内植え込み型HeartMate-VEと最大の内科的治療の成績を比較する二重盲検試験（REMATCH study）が行われ，HeartMate-VE装着患者の成績が図5に示すように2年後において良好であったと報告された[6]。この結果を受けて，米国では2003年秋から心臓移植適応外の重症心不全患者に対するdestination therapyとして認められるようになっており，今後の動向が注目されている。

さらに，長期安定して補助可能なVASの開発が積極的に行われており，これまで用いられてきた拍動型LVASでの完全植込み型Lion Heartの臨床応用が開始されている。また，流入弁および流出弁を必要としないため小型化および長期耐久性が期待される無拍動流型LVASの開発も進められており，軸流ポンプによるJarvik 2000，DeBakey VAD，Incorなどの臨床応用が開始されている。さらに，軸流ポンプより耐久性に優れている遠心ポンプとして，わが国で開発されたTermo社のDuraHeart（図6右）はヨーロッパで臨床応用が開始され，SunMedical社のEvaHeart（図6左）のわが国での臨床治験の準備が進められている。

おわりに

VASは心機能の代行を長期行うことが可能なシステムであり，他の治療法の限界を超えた重症心不全例に対し適応を考慮すべきである。また，心臓移植の代替治療手段として期待されており，今後の新たなVASの臨床導入が望まれる。

文　献

1) Takano H, Nakatani T: Ventricular assist systems: Experience in Japan with Toyobo pump and Zeon Pump. Ann Thorac Surg 61: 317-322, 1996
2) 中谷武嗣，花谷彰久，宮武邦夫，他：人工心臓と心臓移植．循環器専門医 9：51-56，2001
3) 中谷武嗣：レシピエント管理（待機から移植へ）外科管理．循環器病専門医 10：307-312，2003
4) 慢性心不全治療ガイドライン Jpn Circ J 64(suppl 4)：1023-1079, 2000
5) 中谷武嗣：重症心不全の抗凝固，抗血栓療法（補助循環を含む）．ICU と CCU 28：909-913，2004
6) Rose EA, Gelijins AC, Moskowitz AJ, et al: Long-term use of a left ventricular assist device for end-stage heart failure. N Engl J Med 345: 1435-1443, 2001

Abstract

Ventricular Assist System

Takeshi Nakatani and Akihisa Hanatani

Department of Organ Transplantation, National Cardiovascular Center
5-7-1 Fujishirodai, Suita-shi, Osaka 565-8565, Japan

Ventricular assist system (VAS) has been developed to assist cardiac function in severe heart failure patients. Two types of VAS, extracroporeal type and implantable type, are used clinically. VAS can provide long-term support until bridge to recovery or bridge to transplantation. In selection of candidates for VAS, not only hemodynamic parameters but also major organ functions are important factors. Anticoagulation and antithrombotic therapy and prevention of infection are the key issues in patient care with VAS for long-term support. Weaned cases from LVAS and successfully transplanted bridge to transplantation cases are reported in Japanese patients and destination therapy for end-staged heart failure patients is started in western countries. New small and durable VASs are desired in clinical fields and several new VASs are in clinical trails.

ICU & CCU 29(4):265～273, 2005

STEM CELLS
STEM CELL GENETICS AND GENOMICS

Effect of Hypoxia on Gene Expression of Bone Marrow-Derived Mesenchymal Stem Cells and Mononuclear Cells

SHUNSUKE OHNISHI,[a] TAKESHI YASUDA,[b] SOICHIRO KITAMURA,[c] NORITOSHI NAGAYA[a]

Departments of [a]Regenerative Medicine and Tissue Engineering and [c]Cardiovascular Surgery, National Cardiovascular Center, Osaka, Japan; [b]GeneticLab Company, Ltd., Sapporo, Japan

Key Words. Microarray • Mononuclear cell • Mesenchymal stem cell • Hypoxia • Bone marrow

ABSTRACT

MSC have self-renewal and multilineage differentiation potential, including differentiation into endothelial cells and vascular smooth muscle cells. Although bone marrow-derived mononuclear cells (MNC) have been applied for therapeutic angiogenesis in ischemic tissue, little information is available regarding comparison of the molecular foundation between MNC and their MSC subpopulation, as well as their response to ischemic conditions. Thus, we investigated the gene expression profiles between MSC and MNC of rat bone marrow under normoxia and hypoxia using a microarray containing 31,099 genes. In normoxia, 2,232 (7.2%) and 2,193 genes (7.1%) were preferentially expressed more than threefold in MSC and MNC, respectively, and MSC expressed a number of genes involved in development, morphogenesis, cell adhesion, and proliferation, whereas various genes highly expressed in MNC were involved in inflammatory response and chemotaxis. Under hypoxia, 135 (0.44%) and 49 (0.16%) genes were upregulated (>threefold) in MSC and MNC, respectively, and a large number of those upregulated genes were involved in glycolysis and metabolism. Focusing on genes encoding secretory proteins, the upregulated genes in MSC under hypoxia included several molecules involved in cell proliferation and survival, such as vascular endothelial growth factor-D, placenta growth factor, pre-B-cell colony-enhancing factor 1, heparin-binding epidermal growth factor-like growth factor, and matrix metalloproteinase-9, whereas the upregulated genes in MNC under hypoxia included proinflammatory cytokines such as chemokine (C-X-C motif) ligand 2 and interleukin-1α. Our results may provide information on the differential molecular mechanisms regulating the properties of MSC and MNC under ischemic conditions. STEM CELLS *2007;25:1166–1177*

Disclosure of potential conflicts of interest is found at the end of this article.

INTRODUCTION

MSC possess multipotency and terminally differentiate into osteoblasts, chondrocytes, neurons, skeletal muscle cells, endothelial cells, and vascular smooth muscle cells [1, 2]. MSC can be easily isolated from bone marrow-derived mononuclear cells (MNC) and expanded in vitro >1 million-fold. Thus, these features make MSC an attractive therapeutic tool [1]. Although bone marrow-derived MNC have already been established as a tool for cell therapy and have been shown to induce therapeutic neovascularization in critical limb ischemia and myocardial infarction [3–6], MNC transplantation requires harvesting a large number of cells, and some patients are refractory to MNC therapy [7, 8]. We have previously demonstrated that MSC transplantation caused great improvement in rat hind limb ischemia and dilated cardiomyopathy [9, 10]. Recent studies suggest that MSC exert tissue regeneration through paracrine effects, as well as through differentiation into specific cell types [11, 12]. However, the molecular mechanisms that explain the difference between bone marrow-derived MNC and their MSC subpopulation exposed into ischemic conditions are yet to be studied. Thus, the purposes of this study were (a) to compare the gene expression profile of two fractions of clinically applicable bone marrow-derived cells (i.e., freshly isolated MNC versus their cultured MSC subpopulation), and (b) to investigate the effect of hypoxia on gene expression in MSC and MNC.

MATERIALS AND METHODS

Expansion of MSC and Isolation of MNC

Isolation and expansion of MSC were performed as described previously [13]. Briefly, bone marrow cells were isolated from male Lewis rats weighing 220–250 g by flushing out the femoral and tibial cavities with phosphate-buffered saline and plated onto 10-cm dishes in complete culture medium: α-minimal essential medium (Invitrogen, Carlsbad, CA, http://www.invitrogen.com), 10% fetal bovine serum (Invitrogen), 100 U/ml penicillin, and 100 μg/ml streptomycin (Invitrogen). Five days after plating, nonadherent cells were removed, and adherent cells were further propagated for 4–5 passages. These cells were previously demonstrated to be positive for CD29 and CD90 surface markers and negative for CD34 and CD45 [10]. MNC were isolated from whole bone marrow cells by density gradient centrifugation (Histopaque-1083; Sigma-Aldrich, St. Louis, http://www.sigmaaldrich.com). The Animal Care Committee of the National Cardiovascular Center approved the experimental protocol.

Correspondence: Noritoshi Nagaya, M.D., Ph.D., Department of Regenerative Medicine and Tissue Engineering, National Cardiovascular Center, 5-7-1 Fujishirodai, Osaka 565-8565, Japan. Telephone: 81-6-6833-5012; Fax: 81-6-6833-9865; e-mail: nnagaya@ri.ncvc.go.jp; or Shunsuke Ohnishi, M.D., Ph.D., Department of Regenerative Medicine and Tissue Engineering, National Cardiovascular Center, 5-7-1 Fujishirodai, Osaka 565-8565, Japan. Telephone: 81-6-6833-5012; Fax: 81-6-6833-9865; e-mail: sonishi@ri.ncvc.go.jp Received June 6, 2006; accepted for publication February 1, 2007; first published online in STEM CELLS *EXPRESS* February 8, 2007; available online without subscription through the open access option. 1066-5099/2007/$30.00/0 doi: 10.1634/stemcells.2006-0347

Table 1. Primer pairs designed for semiquantitative and quantitative reverse transcription-polymerase chain reaction

Target	Sense primer	Antisense primer
Semiquantitative		
AM	5′-gtggaataagtgggcgctaa-3′	5′-agggctgatcttgtttctgg-3′
COL3A1	5′-cgagattaaagcaagaggaa-3′	5′-gaggcttctttacataccac-3′
CXCL2	5′-tcctcaatgctgtactggtcc-3′	5′-atgttcttcctttccaggtc-3′
HB-EGF	5′-tcccactggaaccacaaaccag-3′	5′-cccacgatgacaagaagacagac-3′
IL-1α	5′-cgcttgagtcggcaaagaaatc-3′	5′-cacatgccatgcgagtgattag-3′
MIF	5′-caccatgcctatgttcatcgtgaaca-3′	5′-cggttccaccttcgcttgagcccggg-3′
MMP-9	5′-aaatgtgggtgtacacaggc-3′	5′-ttcacccggttgtggaaact-3′
MMP-14	5′-agtgccctatgcctacatcc-3′	5′-aatgggcattgggtatccgt-3′
PBEF1	5′-ttggttctggtggcgctttgctac-3′	5′-aaggtccctgctggtgtcctatgt-3′
PGF	5′-acagaaatggaagtggtg-3′	5′-ggctaataaatagagggtagg-3′
SERPINE1	5′-accctcagcatgttcattgc-3′	5′-ctcgttcacctcgatcttgac-3′
SERPINF1	5′-tcaccaaccctgacatccacag-3′	5′-actgccccttgaagtaagccac-3′
SERPINH1	5′-gggcaggatatgccaaggag-3′	5′-gttggcagtgcagatcggaa-3′
VEGF-A	5′-actggaccctggctttactc-3′	5′-acgcactccagggcttcatc-3′
VEGF-D	5′-tccaaacagctctttgagatatcag-3′	5′-ctccaggacatggtgctttaca-3′
GAPDH	5′-tgaaggtcggtgtcaacggatttggc-3′	5′-catgtaggccatgaggtccaccac-3′
Quantitative		
AM	5′-cctttcagcagggtatcgg-3′	5′-cacttattccacttctttcg-3′
CXCL2	5′-gccaccaaccatcagggtac-3′	5′-ccaggtcagttagccttgcct-3′
HB-EGF	5′-ctgagatggcggttccttaca-3′	5′-aggcccagtcagggtagca-3′
IL-1α	5′-agtcactcgcatggcatgtg-3′	5′-atatgtcgggctggttccac-3′
MIF	5′-gaaccgcaactacagcaagct-3′	5′-tggctgcgttcatgtcgtaa-3′
MMP-9	5′-ggcctatttctgccatgacaaatac-3′	5′-ctgcaccgctgaagcaaaag-3′
PBEF1	5′-ttggttctggtggcgctttgctac-3′	5′-aaggtccctgctggtgtcctatgt-3′
PGF	5′-catggactttgaccactgc-3′	5′-caagagaatctggcttggc-3′
VEGF-A	5′-acgaaagcgcaagaaatccc-3′	5′-ttaactcaagctgcctcgcc-3′
VEGF-D	5′-acaagatgagaatccactgcctgg-3′	5′-ctccaggacatggtgctttacaga-3′
GAPDH	5′-gttcttcaatacgtcagacattcg-3′	5′-cattatctttgctgtcacaagagc-3′

Culture of MSC and MNC Under Hypoxia

MSC and MNC (3×10^6 cells) were plated on 10-cm dishes in complete culture medium and incubated under normoxia (21% O_2, 5% CO_2) or hypoxia (1% O_2, 5% CO_2) for 24 hours. For time-dependent hypoxia experiments, cells were incubated for the desired time at 1% O_2. For the experiments with various O_2 levels, cells were incubated under the desired level of O_2 (1%, 3%, 10%, and 20%) for 24 hours.

Microarray Analysis

Total RNA was extracted from cells using an RNeasy Mini Kit (Qiagen, Hilden, Germany, http://www1.qiagen.com) according to the manufacturer's instructions. RNA was quantified by spectrometry, and the quality was confirmed by gel electrophoresis. Double-stranded cDNA was synthesized from 10 μg of total RNA, and in vitro transcription was performed to produce biotin-labeled cRNA using GeneChip One-Cycle Target Labeling and Control Reagents (Affymetrix, Santa Clara, CA, http://www.affymetrix.com) according to the manufacturer's instructions. After fragmentation, 10 μg of cRNA was hybridized with GeneChip Rat Genome 230 2.0 Array (Affymetrix) containing 31,099 genes. GeneChips were then scanned in a GeneChip Scanner 3000 (Affymetrix). Normalization, filtering, and Gene Ontology analysis of the data were performed with GeneSpring GX 7.3.1 software (Agilent Technologies, Palo Alto, CA, http://www.agilent.com). The raw data from each array were normalized as follows: each CEL file was preprocessed with robust multichip average, and each measurement for each gene was divided by the 50th percentile of all measurements. Genes with a change of at least threefold were then selected.

Semiquantitative Reverse Transcription-Polymerase Chain Reaction

Total RNA was extracted from separately prepared cells as described above, and 5 μg of total RNA was reverse-transcribed into cDNA using avian myeloblastosis virus transcriptase (Ambion, Austin, TX, http://www.ambion.com) and oligo(dT) primers. Polymerase chain reaction (PCR) amplification was performed in 50 μl containing 1 μl of cDNA and 2.5 U of Taq DNA polymerase (Takara, Otsu, Japan, http://www.takara.co.jp). The oligonucleotides used in semiquantitative reverse transcription (RT)-PCR analysis are listed in Table 1. Glyceraldehyde-3-phosphate dehydrogenase (GAPDH) mRNA amplified from the same samples served as an internal control. PCR mixtures were denatured at 95°C for 5 minutes, and cDNA templates were amplified as follows: 25 cycles (21 cycles for GAPDH) of denaturation at 95°C for 1 minute, annealing at 45–55°C for 45 seconds, and extension at 72°C for 1 minute. At the end of the cycling, the samples were incubated at 72°C for 10 minutes. The amplified DNA products were visualized on 2% agarose gels and photographed under ultraviolet light.

Quantitative Real-Time RT-PCR

PCR amplification was performed in 50 μl containing 1 μl of cDNA and 25 μl of Power SYBR Green PCR Master Mix (Applied BioSystems, Foster City, CA, http://www.appliedbiosystems.com). The oligonucleotides used in quantitative real-time RT-PCR analysis are listed in Table 1. GAPDH mRNA amplified from the same samples served as an internal control. After an initial denaturation at 95°C for 10 minutes, a 2-step cycle procedure was used (denaturation at 95°C for 15 seconds, annealing and extension at 60°C for 1 minute) for 40 cycles in a 7700 sequence detector (Applied Biosystems). Gene expression levels were normalized according to that of GAPDH and compared with that at normoxia (20% O_2). The data were analyzed with Sequence Detection Systems software (Applied BioSystems).

RESULTS

Reproducibility of Microarray Experiments

Reproducibility in the microarray experiment was assessed by repeated experiments using separately prepared RNAs. The correlation coefficient between two microarray data sets obtained from repeated experiments was greater than 0.98 for all

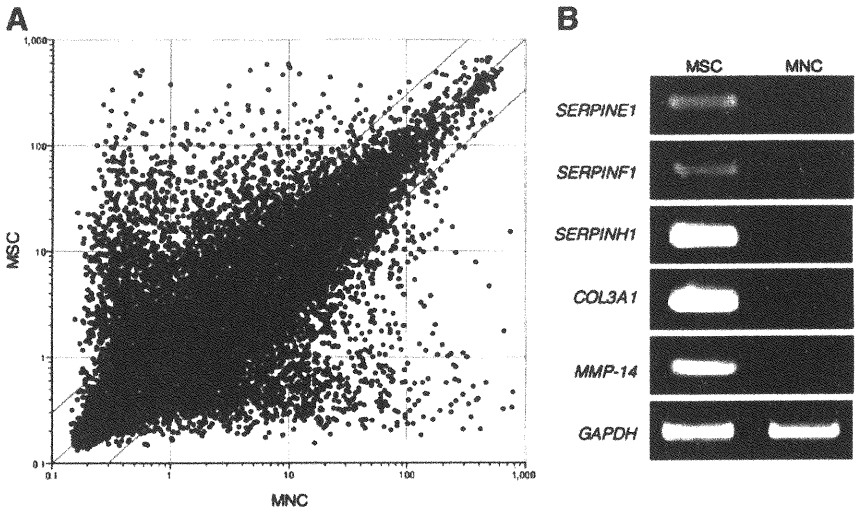

Figure 1. Expression profile of bone marrow-derived MSC versus MNC. **(A):** Normalized microarray data sets of MSC and MNC. All 31,099 gene probes are represented in this plot. The outer lines indicate a threefold difference, whereas the central line represents equality. **(B):** Semiquantitative reverse transcription-polymerase chain reaction of selected genes from Table 2, including serine protease inhibitors. GAPDH was used as an internal control. Abbreviations: GAPDH, glyceraldehyde-3-phosphate dehydrogenase; MNC, mononuclear cell.

gene probes, indicating that the whole experimental procedure was highly reproducible (data not shown).

Differentially Expressed Genes in Bone Marrow-Derived MSC and MNC Under Normoxia

Of 31,099 genes analyzed, 2,232 genes (7.2%) were highly expressed (>threefold) in MSC (Fig. 1A) and 55 genes (0.18%) were highly expressed more than 100-fold (Table 2), whereas 2,193 genes (7.1%) were highly expressed (>threefold) in MNC, and 69 genes (0.22%) were highly expressed more than 100-fold (Table 3). Noteworthy, the highly expressed genes in MSC (>threefold) included various types of molecules involved in biogenesis of extracellular matrix, such as collagens (Iα1, Iα2, IIIα1, IVα1, IVα2, Vα1, Vα2, VIα2, VIα3, VIIIα1, VIIIα2, XIα1, XIIα1, XIVα1, XV, XVIα1, and XVIIIα1), matrix metalloproteinases (MMP-2, -12, -14, -16, -19, and -23), serine proteases (PRSS9, 11, 23, and 35), and serine protease inhibitors (SERPINE1, SERPINF1, and SERPINH1). To verify the gene expression profile determined by our microarray analysis, the expression levels of serine protease inhibitors (SERPINE1, SERPINF1, and SERPINH1), COL3A1, and MMP-14 were analyzed by semiquantitative RT-PCR, using total RNAs separately obtained from MSC and MNC (Fig. 1B). The results showed that the differential expression pattern was in good agreement with that from the microarray analysis.

Functional Classification of Highly Expressed Genes in MSC and MNC Under Normoxia

To evaluate the enriched genes in MSC, a total of 2,232 highly represented genes (>threefold) were classified by functional annotation using gene ontology terms (Table 4). Nineteen terms in the list had a p value of less than .0001, including development (e.g., transgelin, actin-γ1, and short stature homeobox-2), morphogenesis (e.g., bone morphological protein-2, transforming growth factor-β3, and fibrillin-2), cell adhesion (e.g., melanoma cell adhesion molecule, neural cell adhesion molecule-1, and cadherin-11), and cell proliferation (e.g., connective tissue growth factor, fibroblast growth factor-7, and platelet-derived growth factor-A). On the other hand, for MNC, there were 30 listed terms from 2,193 enriched genes with a p value of less than .0001, including hemopoiesis, inflammatory response, and chemotaxis (Table 4).

Differentially Upregulated Genes in Bone Marrow-Derived MSC and MNC in Response to Hypoxia

To investigate the difference in gene expression in response to hypoxia, microarray analysis was performed using total RNAs obtained from MSC and MNC incubated under hypoxia for 24 hours (Fig. 2A; Tables 5 and 6). The results demonstrated that 135 (0.44%) and 49 (0.16%) genes were upregulated (>threefold) in MSC and MNC under hypoxia, respectively (Fig. 2B), and a significant number of those upregulated genes were involved in glycolysis and metabolism, according to gene ontology classification (data not shown). However, focusing on genes encoding secretory proteins, the upregulated genes in MSC under hypoxia included several molecules involved in cell proliferation and survival, such as vascular endothelial growth factor-D (*VEGF-D*), placenta growth factor (*PGF*), pre-B-cell colony-enhancing factor 1 (*PBEF1*), heparin binding epidermal growth factor-like growth factor (*HB-EGF*), and matrix metalloproteinase-9 (*MMP-9*), whereas the upregulated genes in MNC included some proinflammatory cytokines, such as chemokine (C-X-C motif) ligand 2 (*CXCL2*) and interleukin-1α (*IL-1α*) (Fig. 2B). Pairwise comparison of those upregulated genes from both MSC and MNC revealed that only 29 genes overlapped (21.3% in MSC and 59.2% in MNC), including *VEGF-A*, adrenomedullin (*AM*), and macrophage migration inhibitory factor (*MIF*) (Fig. 2B). Semiquantitative RT-PCR for those upregulated genes encoding secretory proteins confirmed the consistency of microarray data (Fig. 2C). To follow the kinetics of those upregulated genes, cells were cultured under different time points at 1% O_2 or different grades of hypoxia, and quantitative real-time RT-PCR was performed. The results demonstrated that the time course and sustainability of gene expression were differently regulated (Fig. 2D). The expression of all genes except *AM* was gradually increased in MSC under hypoxia, whereas *AM* expression was peaked at 12 hours and slightly decreased at 24 hours. On the other hand, the expression of *MIF*, *VEGF-A*, and *AM* in MNC were peaked at 6 hours and was sustained up to 24 hours, whereas the expression of *IL-1α* and *CXCL2* was gradually increased. When cells were cultured at different O_2 levels for 24 hours, most of the genes except *VEGF-D* were upregulated even at 10% O_2 in MSC, whereas the expression of three (*MIF*, *IL-1α*, and *CXCL2*) in MNC was unaffected at 10% O_2 and reached a peak at 1% O_2 (Fig. 2E).

Table 2. Genes upregulated in MSC (>100-fold)

Gene name	GenBank accession no.	Fold change
Collagen, type III, α1 (*COL3A1*)	**BI275716**	**979.7**
Transgelin (*TAGLN*)	NM_031549	918.1
Lysyl oxidase (*LOX*)	**NM_017061**	**910.5**
Follistatin-like 1 (*FSTL1*)	BG665037	689.4
Steroid sensitive gene 1 (*SSG1*)	**AI235465**	**563.7**
Collagen, type V, α2 (*COL5A2*)	AI179399	557.3
Actin, γ2 (*ACTG2*)	**NM_012893**	**486.8**
Protease, serine, 23 (*PRSS23*)	AI177099	427.2
Strongly similar to NP_035737.1 tenascin C (*TNC*)	**AI176034**	**394.1**
Serine proteinase inhibitor, clade H, member 1 (*SERPINH1*)	BI285495	379.7
Protein kinase C, δ binding protein (*PRKCDBP*)	**NM_134449**	**352.3**
Syndecan 2 (*SDC2*)	BG668421	315.5
Caveolin (*CAV*)	**BI285449**	**313.6**
Heat shock protein 1 (*HSPB1*)	NM_031970	312.8
Lysyl oxidase-like 2 (predicted)	**AI044651**	**307.4**
FAT tumor suppressor (*Drosophila*) homolog (*FATH*)	NM_031819	295.2
Protease, serine, 11 (*PRSS11*)	**NM_031721**	**284.7**
Arginase 1 (*ARG1*)	NM_017134	243.0
Cysteine knot superfamily 1, BMP antagonist 1 (*CKTSF1B1*)	**NM_019282**	**231.9**
Serine proteinase inhibitor, clade F, member 1 (*SERPINF1*)	AI179984	228.4
Serine proteinase inhibitor, clade E, member 1 (*SERPINE1*)	**NM_012620**	**218.5**
Nidogen (*NID*)	AI235948	214.4
Matrix metalloproteinase 14 (*MMP14*)	**X83537**	**211.7**
Lumican (*LUM*)	NM_031050	205.8
Transforming growth factor, β3 (*TGFB3*)	**NM_013174**	**193.5**
Cadherin 11 (*CDH11*)	BI296340	189.0
Par-4 (*PAWR*)	**U05989**	**181.0**
Collagen, type XI, α1 (*COL11A1*)	BM389291	179.1
Peptidylprolyl isomerase C (*PPIC*)	**BI291292**	**170.5**
A disintegrin and metalloproteinase with thrombospondin motifs 1 (*ADAMTS1*)	NM_024400	165.8
Interleukin 1 receptor-like 1 (*IL1RL1*)	**NM_013037**	**153.9**
WNT1 inducible signaling pathway protein 2 (*WISP2*)	NM_031590	153.3
Glypican 1 (*GPC1*)	**NM_030828**	**150.0**
Gap junction membrane channel protein α1 (*GJA1*)	AI411352	138.0
Matrix metalloproteinase 2 (*MMP2*)	**U65656**	**131.2**
Caldesmon 1 (CALD1)	BI291848	128.2
Growth factor receptor bound protein 14 (*GRB14*)	**NM_031623**	**128.1**
Coagulation factor 3 (*F3*)	NM_013057	127.1
Four and a half LIM domains 1 (*FHL1*)	**BI298356**	**126.9**
Calponin 1 (*CNN1*)	NM_031747	124.2
Tissue inhibitor of metalloproteinase 1 (*TIMP1*)	**NM_053819**	**119.9**
Strongly similar to NP_035711.1 thrombospondin 2 (*TSP-2*)	BF408413	119.4
Secreted acidic cysteine rich glycoprotein (*SPARC*)	**NM_012656**	**118.7**
Plastin 3 (*PLS3*)	BG672591	117.7
Superoxide dismutase 3 (*SOD3*)	**NM_012880**	**116.4**
Arginine vasopressin receptor 1A (*AVPR1A*)	NM_053019	114.7
Melanoma antigen, family D, 1 (*MAGED1*)	**NM_053409**	**114.2**
Tight junction protein 1 (*TJP1*)	AW434048	113.2
Connective tissue growth factor (*CTGF*)	**NM_022266**	**109.8**
LIM domain only protein 7 (*LMO7*)	AI598833	107.6
Tumor necrosis factor receptor superfamily, member 12a (*TNFRSF12A*)	**BI303379**	**104.2**
Actin, α1 (*ACTA1*)	NM_019212	104.2
Heart fatty acid binding protein 3 (*FABP3*)	**NM_024162**	**103.8**
Transforming growth factor, β2 (*TGFB2*)	BF420705	103.5
Short stature homeobox 2 (*SHOX2*)	**NM_013028**	**101.4**

DISCUSSION

In this study, we focused on differential gene expression of freshly isolated MNC and their cultured MSC subpopulation and the effect of hypoxia on gene expression of those cells. We showed that (a) MSC preferentially expressed a large number of genes involved in development, morphogenesis, cell adhesion, and cell proliferation, whereas MNC expressed various genes involved in inflammatory response and chemotaxis, and (b) MSC and MNC responded to hypoxia mostly in a distinct manner; several genes involved in cell proliferation and survival were upregulated in MSC, whereas some proinflammatory cytokines were upregulated in MNC.

In normoxia, MSC highly expressed various types of molecules that are considered to be essential for development and morphogenesis. Notably, the enriched genes in MSC included a number of molecules involved in biogenesis of extracellular matrix, such as collagens, MMPs, serine proteases, and serine protease inhibitors. MNC, on the other hand, highly expressed a large number of molecules involved in inflammatory response and chemotaxis. This result is largely consistent with a recent

Table 3. Genes upregulated in MNC (>100-fold)

Gene name	GenBank accession no.	Fold change
Hemoglobin α2 chain (*HBA-A1*)	AI179404	2,303
S100 calcium binding protein A9 (*S100A9*)	NM_053587	2,007
Hemoglobin β chain complex (*HBB*)	BI287300	1,996
Defensin Rat NP-3 precursor (*NP3B*)	U16683	1,439
S100 calcium binding protein A8 (*S100A8*)	NM_053822	1,274
Defensin Rat NP-4 precursor (*NP4*)	U16684	974.3
Ficolin B (*FCNB*)	NM_053634	813.6
Similar to Igh-6 protein (*IGH-6*)	AA996557	774.4
Mast cell protease 8 (*MCPT8*)	NM_021598	698.4
Chemokine (C-X-C motif) receptor 4 (*CXCR4*)	AA945737	694.5
Robo-1 (*ROBO-1*)	NM_031537	603.6
Carbonic anhydrase I (predicted)	BM383006	508.5
Serine (or cysteine) proteinase inhibitor, clade B, member 10 (*SERPINB10*)	BF399855	476.6
Similar to Ig heavy chain V-III region VH26 precursor (*IGHA*)	AI412189	459.9
Pre-eosinophil-associated ribonuclease-2	AI177934	430.9
Mast cell protease 9 (*MCPT9*)	NM_019323	409.6
Napsin A aspartic peptidase (*NAPSA*)	NM_031670	371.8
CD74 antigen (*CD74*)	NM_013069	369.3
Immunoglobulin joining chain (predicted)	AA817898	356
Mast cell protease 10 (*MCPT10*)	X68657	354.5
Similar to Myb proto-oncogene protein (*C-MYB*)	AI234125	341.6
Carbonic anhydrase 2 (*CA2*)	NM_019291	340.6
CD69 antigen (*CD69*)	AI137672	325.2
GDP dissociation inhibitor (*GDI*) β (predicted)	BF285771	321.8
Defensin, α5 (*DEFA*)	U16686	318.7
CD24 antigen (*CD24*)	BI285141	315.2
Transferrin (*TF*)	AA945178	269.8
CD37 antigen (*CD37*)	NM_017124	261.8
Cathepsin E (*CTSE*)	NM_012938	252.6
Coronin, actin binding protein 1A (*CORO1A*)	NM_130411	219.4
Lysosomal-associated protein transmembrane 5 (*LAPTM5*)	NM_053538	215.4
Macrophage expressed gene 1 (*MPEG1*)	AI170394	215.3
Protein tyrosine phosphatase, receptor type, C (*PTPRC*)	BF288130	207.5
Arginosuccinate synthetase (*AS*)	BF283456	205.1
Nuclear factor, erythroid derived 2 (predicted)	AW252129	198.2
Fibrinogen-like 2 (*FGL2*)	AI716194	197
Cytochrome b-245, β polypeptide (*CYBB*)	BE098739	196.7
Similar to RIKEN cDNA 1100001H23 (predicted)	BI285951	183.2
Leukocyte immunoglobulin-like receptor, subfamily B, member 3 (predicted)	AF169637	174
Matrix metallopeptidase 8 (*MMP8*)	NM_022221	173.6
CD53 antigen (*CD53*)	NM_012523	171.2
Complement component 3 (*C3*)	NM_016994	169.6
Aminolevulinic acid synthase 2 (*ALAS2*)	NM_013197	164.8
Similar to FCRL (predicted)	AI408164	163.4
Mast cell antigen 32 (*MCA32*)	NM_021585	161.2
Interleukin 1 receptor, type II (*IL1R2*)	NM_053953	161.2
Membrane-spanning 4-domains, subfamily A, member 1 (predicted)	AA817742	160.6
CD79B antigen (*CD79B*)	NM_133533	159.2
Homeobox only domain (*HOD*)	NM_133621	153.2
Chemokine (C-C motif) ligand 6 (*CCL6*)	BE095824	150.7
Similar to regulator of Fas-induced apoptosis	AI410062	148.3
RT1 class II, locus Bb (*RT1-BB*)	AI715202	146.2
Immunoglobulin superfamily, member 6 (*IGSF6*)	NM_133542	137.3
Pre-B lymphocyte gene 3 (predicted)	AW524266	130.9
Proteoglycan 2, bone marrow (*PRG2*)	NM_031619	126.5
Similar to GARP protein precursor (*GARPIN*) (predicted)	BM388665	125.4
Erythroid associated factor (predicted)	AI230287	124.6
Neurofibromatosis 1 (*NF1*)	BM386570	124
Similar to Rho GTPase activating protein 15	AI178168	123.1
RAS-related C3 botulinum substrate 2 (predicted)	AI010476	117.2
Natural killer cell group 7 sequence (*NKG7*)	NM_133540	113.2
Chemokine (C-X-C motif) ligand 2 (*CXCL2*)	NM_053647	112.3
Chymase 1, mast cell (*CMA1*)	NM_013092	108.8
Ras homolog gene family, member H (predicted)	AI012081	106.4
Similar to Clecsf12 protein	AI045955	105.8
Similar to protein tyrosine phosphatase 20	AW916153	105.1
Chemokine (C-C motif) receptor 2 (*CCR2*)	NM_021866	104.6
Solute carrier family 4, member 1 (*SLC4A1*)	BE113640	103.7
Thyroglobulin (*TG*)	AI500952	102.8

Abbreviation: MNC, mononuclear cells.

Table 4. Classification of highly expressed genes in MSC and MNC (>threefold) according to gene ontology terms

Category	% of genes in category	% of genes in list in category	*p* value
MSC			
0007275: development	23.2	35.8	1.1×10^{-12}
0007155: cell adhesion	5.7	12.7	5.1×10^{-11}
0048513: organ development	10.6	19.1	2.6×10^{-10}
0009653: morphogenesis	9.4	16.5	2.4×10^{-8}
0008283: cell proliferation	6.1	11.2	1.0×10^{-6}
0001501: skeletal development	2.1	5.3	1.2×10^{-6}
0016049: cell growth	1.8	4.8	1.3×10^{-6}
0009887: organ morphogenesis	5.0	9.5	2.3×10^{-6}
0008610: lipid biosynthesis	2.4	5.7	3.2×10^{-6}
0040007: growth	2.5	5.7	5.4×10^{-6}
0016125: sterol metabolism	1.1	3.3	6.8×10^{-6}
0009888: tissue development	2.6	5.9	7.2×10^{-6}
0016126: sterol biosynthesis	0.5	2.2	8.5×10^{-6}
0000074: regulation of progression through cell cycle	4.6	8.6	1.2×10^{-5}
0030324: lung development	0.6	2.2	1.3×10^{-5}
0007167: enzyme-linked receptor protein signaling pathway	3.1	6.4	1.4×10^{-5}
0000902: cellular morphogenesis	4.2	7.9	2.2×10^{-5}
0035295: tube development	0.9	2.9	2.4×10^{-5}
0001944: vasculature development	1.4	3.5	8.5×10^{-5}
MNC			
0009607: response to biotic stimulus	8.2	25.5	3.2×10^{-34}
0006952: defense response	8.0	24.9	2.4×10^{-33}
0006955: immune response	7.1	22.8	1.9×10^{-31}
0009611: response to wounding	4.7	12.6	4.3×10^{-13}
0009605: response to external stimulus	7.6	17.0	6.9×10^{-13}
0009613: response to pest, pathogen or parasite	4.6	11.9	2.8×10^{-12}
0006954: inflammatory response	2.5	7.3	3.3×10^{-9}
0001775: cell activation	1.6	5.4	5.4×10^{-9}
0006935: chemotaxis	1.5	5.0	3.1×10^{-8}
0006950: response to stress	10.7	18.6	4.0×10^{-8}
0048534: hemopoietic or lymphoid organ development	1.4	4.6	3.0×10^{-7}
0030097: hemopoiesis	1.4	4.6	3.0×10^{-7}
0030593: neutrophil chemotaxis	0.3	2.1	3.7×10^{-7}
0006968: cellular defense response	1.0	3.6	1.2×10^{-6}
0050874: organismal physiological process	23.0	32.0	1.2×10^{-6}
0050900: immune cell migration	0.5	2.5	1.3×10^{-6}
0006909: phagocytosis	0.4	2.1	1.5×10^{-6}
0030595: immune cell chemotaxis	0.5	2.3	2.6×10^{-6}
0050766: positive regulation of phagocytosis	0.2	1.5	4.6×10^{-6}
0046649: lymphocyte activation	1.3	4.0	5.4×10^{-6}
0001816: cytokine production	0.5	2.3	6.7×10^{-6}
0050778: positive regulation of immune response	0.6	2.5	7.7×10^{-6}
0030098: lymphocyte differentiation	0.6	2.5	1.1×10^{-5}
0042110: T-cell activation	0.9	2.9	2.5×10^{-5}
0045807: positive regulation of endocytosis	0.2	1.5	2.6×10^{-5}
0045576: mast cell activation	0.1	1.0	3.3×10^{-5}
0006911: phagocytosis, engulfment	0.1	1.0	3.3×10^{-5}
0030217: T-cell differentiation	0.4	1.9	6.5×10^{-5}
0001810: regulation of type I hypersensitivity	0.1	0.8	6.7×10^{-5}
0009617: response to bacteria	0.5	2.1	7.0×10^{-5}

Abbreviation: MNC, mononuclear cells.

report by Silva et al., which compared the gene expression of bone marrow-derived MSC with that of $CD34^+$ hematopoietic precursors by serial analysis of gene expression [14]. Recently, the differential gene expression profile of human umbilical cord blood (UCB)-derived MNC compared with their MSC subpopulation has been reported, and many of the genes listed as highly represented in UCB-derived MSC were identical to our results obtained from adult rat bone marrow [15]. Others have compared the gene expression profile of MSC with that of fibroblasts [16, 17]. However, there is no report regarding the gene expression profile of bone marrow-derived MSC, which are more relevant to clinical settings as a therapeutic tool than UCB-derived MSC, in comparison with bone marrow-derived MNC, which have already been applied for regenerative medicine [3–6]. Our results may provide information on the differential molecular mechanisms regulating the properties of bone marrow-derived MNC and their MSC subpopulation.

We have recently reported that MSC, in comparison with MNC, supplied larger amounts of angiogenic, antiapoptotic, and mitogenic factors such as VEGF, AM, hepatocyte growth factor and insulin-like growth factor-1, and some of the transplanted MSC survived even in an ischemic environment [9, 10]. Recent studies from other groups indicate that MSC mediate pleiotropic effects by secreting a large number of growth factors, antiapoptotic factors, and cytokines [11, 12, 18, 19]. Thus, it is of importance to investigate the difference in gene expression

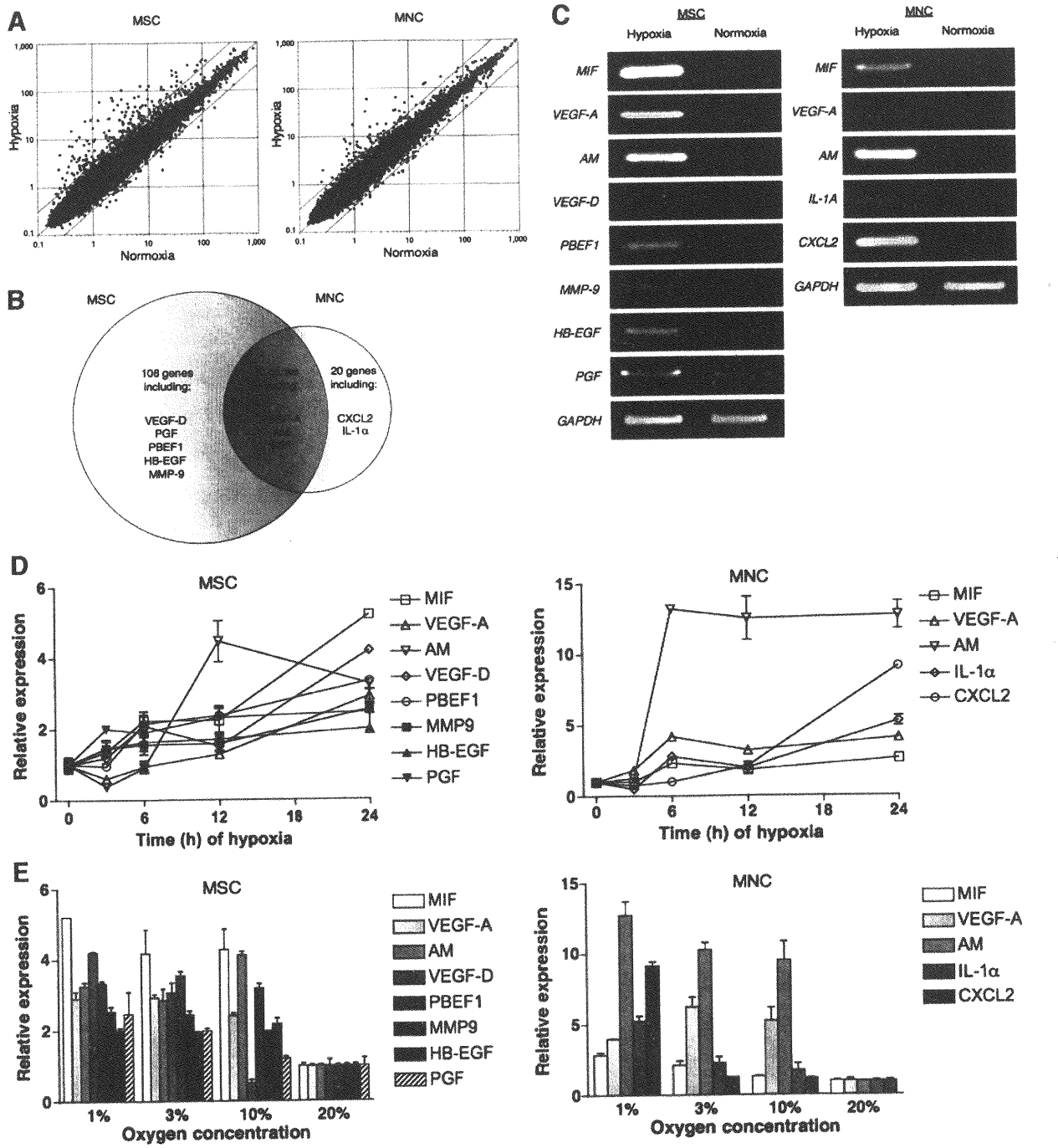

Figure 2. Expression profiles of MSC and MNC under normoxia versus hypoxia. **(A):** Normalized microarray data sets. All 31,099 gene probes are represented in this plot. The outer lines indicate a threefold difference, whereas the central line represents equality. **(B):** Pairwise comparison of upregulated genes from MSC and MNC under hypoxia. The numbers of genes upregulated more than threefold are presented. Gene symbols of selected secretory proteins are provided. **(C):** Semiquantitative reverse transcription-polymerase chain reaction (RT-PCR) of genes encoding secretory proteins listed in **(B)**. **(D):** Quantitative RT-PCR of genes encoding secretory proteins listed in **(B)** at different time points of 1% O_2. All transcription rates were estimated with reference to expression of each gene at normoxia (20% O_2). **(E):** Quantitative RT-PCR of genes encoding secretory proteins listed in **(B)** at different O_2 levels. All transcription rates were estimated with reference to expression of each gene at normoxia (20% O_2). Abbreviations: h, hours; MNC, mononuclear cell.

profile between MSC and MNC under hypoxia, which mimics the ischemic environment in vitro. Our observation revealed that MSC had more than five times as many exclusively upregulated genes as did MNC (106 vs. 20 genes), and only 29 genes, including *VEGF-A*, *AM*, and *MIF*, were commonly upregulated. This result is largely consistent with a very recent report by Martin-Rendon et al., which compared the gene expression of human cord blood $CD133^+$ cells with cultured bone marrow-derived MSC in response to hypoxia [20]. Although they cultured MNC in serum-free medium with cytokines such as IL-6, stem cell factor, Flt3-ligand, and thrombopoietin, the commonly upregulated genes in $CD133^+$ cells and MSC included *VEGF-A* and *AM*, in agreement with our results. MIF has been reported to be upregulated in response to hypoxia in glial tumor cells and

Table 5. Genes upregulated in MSC under hypoxia (>threefold)

Gene name	GenBank accession no.	Fold change
Cytochrome c oxidase, subunit 4b (*COX4B*)	NM_053472	33.2
Neuronal cell death inducible putative kinase (*NIPK*)	AB020967	33.0
ERO1-like (*ERO1L*)	AI146215	31.8
Solute carrier family 2, member 1 (*SLC2A1*)	BI284218	20.4
Serine hydroxymethyl transferase 2 (predicted)	BF411239	19.8
Liver glycogen phosphorylase (*PYGL*)	NM_022268	19.7
ATP-binding cassette, sub-family A (*ABC1*), member 4 (predicted)	AI602131	19.5
Putative ISG12(b) protein	AA819034	18.0
Enolase 2, γ (*ENO2*)	AF019973	17.5
Apelin (*APLN*)	AI177057	16.9
Metallothionein (*MT1A*)	AF411318	13.6
Hypoxia induced gene 1 (*HIG1*)	H31665	13.4
N-myc downstream regulated gene 1 (predicted)	BM384099	13.0
DNA-damage-inducible transcript 4 (*DDIT4*)	NM_080906	12.8
BCL2/adenovirus E1B 19 kDa-interacting protein 3 (*BNIP3*)	NM_053420	12.2
Adenylate kinase 3-like 1 (*AK3L1*)	AA891949	11.8
EGL nine homolog 1 (*EGLN1*)	BI282122	11.2
Similar to eukaryotic translation initiation factor 4E member 3	AI575608	11.0
Heme oxygenase 1 (*HMOX1*)	NM_012580	10.8
Caspase 11 (*CASP11*)	NM_053736	10.8
Similar to glutaminyl-peptide cyclotransferase precursor	BM390001	10.7
Adrenomedullin (*ADM*)	NM_012715	9.5
DNA-damage inducible transcript 3 (*DDIT3*)	NM_024134	9.3
N-myc downstream-regulated gene 2 (*NDRG2*)	NM_133583	9.1
Alcohol dehydrogenase 1 (*ADH1*)	NM_130780	8.8
Vascular endothelial growth factor A (*VEGFA*)	AF080594	8.2
Solute carrier family 16, member 3 (*SLC16A3*)	NM_030834	8.1
Aldolase C (*ALDOC*)	NM_012497	8.0
Stanniocalcin 1 (*STC1*)	BM386683	7.4
Macrophage migration inhibitory factor (*MIF*)	NM_031051	7.4
Phosphoglycerate kinase 1 (*PGK1*)	NM_053291	7.3
Similar to eukaryotic translation initiation factor 4E member 3	AI101338	7.0
Growth and transformation-dependent protein (*LOC60380*)	BE113639	6.8
Pyruvate dehydrogenase kinase 1 (*PDK1*)	NM_053826	6.7
Similar to von Willebrand factor A-domain-containing 1 (predicted)	BF413643	6.7
Procollagen-proline, 2-oxoglutarate 4-dioxygenase, α2 polypeptide (predicted)	BI274349	6.7
Procollagen-proline, 2-oxoglutarate 4-dioxygenase, α1 polypeptide (*P4HA1*)	BI274401	6.3
Asparagine synthetase (*ASNS*)	U07202	6.3
Hexokinase 2 (*HK2*)	BI294137	6.3
Strongly similar to NP_109603.2 glycogen synthase 1	BM392117	6.2
Glucan (1,4-α-), branching enzyme 1 (predicted)	BI284270	6.1
Activating transcription factor 5 (*ATF5*)	BM391471	6.0
Phosphofructokinase (*PFKL*)	NM_013190	5.8
Zinc finger protein 84 (predicted)	BI282114	5.7
Matrix metallopeptidase 9 (*MMP9*)	NM_031055	5.7
Triosephosphate isomerase 1 (*TPI1*)	NM_022922	5.6
CTL target antigen (*CTH*)	NM_017074	5.6
Glutamic pyruvate transaminase 2 (predicted)	AI454322	5.5
Phosphoserine aminotransferase 1 (*PSAT1*)	AI230228	5.4
Prostaglandin E synthase (*PTGES*)	AB048730	5.2
G protein-coupled receptor 128 (predicted)	BM388427	5.2
Rab40b, member RAS oncogene family (predicted)	AA924620	5.0
Inhibitor of DNA binding 2 (*ID2*)	AI008792	5.0
RAD23a homolog (predicted)	BF553981	5.0
Solute carrier family 2 (*SLC2A3*)	AA901341	4.9
Pre-B-cell colony enhancing factor 1 (*PBEF1*)	BI297612	4.8
Neural cell adhesion molecule 1 (*NCAM1*)	AI229409	4.7
Basic helix-loop-helix domain-containing, class B2 (*BHLHB2*)	NM_053328	4.7
Strongly similar to XP_579758.1 (predicted)	AI105202	4.7
Peptidoglycan recognition protein 1 (*PGLYRP1*)	NM_053373	4.6
Growth arrest specific 6 (*GAS6*)	H33111	4.6
Glucose phosphate isomerase (*GPI*)	BI283882	4.5
Cyclin G2 (predicted)	AI408309	4.5
O-Acyltransferase domain-containing 2 (predicted)	BG665934	4.5
Carbonic anhydrase 9 (predicted)	BM391835	4.4
Lactate dehydrogenase A (*LDHA*)	NM_017025	4.4
Similar to neuronal interacting factor X 1 (*NIX1*)	AI511126	4.4
Similar to phosphoglycerate mutase (EC 5.4.2.1) B chain	AI535383	4.4

Continued

Table 5. (continued)

Gene name	GenBank accession no.	Fold change
Phosphofructokinase, platelet (*PFKP*)	**BM389769**	**4.3**
Aldolase A (*ALDOA*)	NM_012495	4.3
Similar to synaptotagmin-like homologue lacking C2 domains-b	**BF410325**	**4.2**
Forkhead box K2 (predicted)	BF551356	4.1
Centaurin, β 1 (predicted)	**BI275873**	**4.1**
Max interacting protein 1 (*MXI1*)	AI409308	4.1
Protease, serine, 15 (*PRSS15*)	**NM_133404**	**4.1**
Phosphoenolpyruvate carboxykinase 2 (predicted)	AI228633	4.0
SNF1-like kinase (*SNF1LK*)	**NM_021693**	**4.0**
Formyltetrahydrofolate synthetase domain-containing 1 (predicted)	BF281848	4.0
Similar to cDNA sequence BC032204 (predicted)	**AI045958**	**3.9**
RAR-related orphan receptor α (predicted)	AI235414	3.9
Phosphoserine phosphatase (predicted) (*PSPH*)	**BF282282**	**3.9**
BM1k MHC class Ib antigen (*BM1*)	AJ243973	3.9
Rab26 (*RAB26*)	**NM_133580**	**3.9**
Cytochrome P450, family 26, subfamily b, polypeptide 1 (*CYP26B1*)	BF397093	3.9
Serine hydroxymethyl transferase 2 (*MGC105820*)	**BF285150**	**3.8**
3-phosphoglycerate dehydrogenase (*PHGDH*)	NM_031620	3.8
Tissue inhibitor of metalloproteinase 3 (*TIMP3*)	**AI599265**	**3.8**
Strongly similar to NP_076005.1 hypoxia-inducible protein 2	BI282296	3.8
Similar to B230212L03Rik protein	**BG670960**	**3.8**
Fatty acid binding protein 5, epidermal (*FABP5*)	U13253	3.7
Glutamyl-prolyl-tRNA synthetase (predicted)	**AI234919**	**3.7**
Very low density lipoprotein receptor (*VLDLR*)	AA849857	3.7
Eukaryotic translation initiation factor 4E binding protein 1 (*EIF4EBP1*)	**NM_053857**	**3.7**
Similar to RIKEN cDNA 2810428C21	BF407585	3.7
Keratin complex 2, basic, gene 8	**BF281337**	**3.6**
Enolase 1, α (*ENO1*)	NM_012554	3.6
Activating transcription factor 4 (*ATF4*)	**NM_024403**	**3.6**
Glutamic pyruvate transaminase (alanine aminotransferase) 2 (predicted)	AA955605	3.6
EGL nine homolog 3 (*EGLN3*)	**NM_019371**	**3.6**
LIM and senescent cell antigen-like domains 2 (predicted)	BI275904	3.6
Pre-mtHSP70	**S75280**	**3.6**
D site albumin promoter binding protein	AI230048	3.6
6-phosphofructo-2-kinase/fructose-2,6-biphosphatase 3 (*PFKFB3*)	**D87247**	**3.5**
Caspase 12 (*CASP12*)	NM_130422	3.5
A disintegrin-like and metalloprotease with thrombospondin type 1 motif, 8 (predicted)	**AI577318**	**3.5**
LOC362671 (predicted)	AI409584	3.4
Histone 2a (*H2A*)	**BE104595**	**3.4**
Phosphoglycerate mutase 1 (*PGAM1*)	NM_053290	3.4
Placental growth factor (*PGF*)	**BF281271**	**3.4**
CCAAT/enhancer binding protein, δ (*CEBPD*)	NM_013154	3.4
Activating transcription factor 3 (*ATF3*)	**NM_012912**	**3.4**
Heat shock protein, A (predicted)	BI282281	3.3
Pyruvate kinase, muscle (*PKM2*)	**NM_053297**	**3.3**
Histone 1, H2ai (predicted)	AI176481	3.3
Similar to RIKEN cDNA E130201N16 (predicted)	**BE113624**	**3.2**
Phosphoglucomutase 1 (*PGM1*)	NM_017033	3.2
Fos-like antigen 1 (*Fosl1*)	**NM_012953**	**3.2**
Growth arrest specific 5 (*GAS5*)	BF287008	3.2
Monoglyceride lipase (*MGLL*)	**BG372713**	**3.2**
Erythropoietin receptor (*EPOR*)	NM_017002	3.2
Solute carrier family 6, member 9 (*SLC6A9*)	**M95413**	**3.2**
Heparin-binding epidermal growth factor-like growth factor (*HB-EGF*)	NM_012945	3.1
Similar to genethonin 1 (predicted)	**BI295979**	**3.1**
Similar to 5830411E10Rik protein (predicted)	BI295501	3.1
Glutamate-cysteine ligase, catalytic subunit (*GCLC*)	**AA892770**	**3.1**
Neuronatin (*NNAT*)	NM_053601	3.1
Neurexophilin 4 (*NXPH4*)	**NM_021680**	**3.1**
Similar to hypothetical protein D4Ertd765e (predicted)	AI172274	3.1
Similar to RIKEN cDNA 4930455F23 (predicted)	**BI281653**	**3.1**
Zinc finger and BTB domain-containing 5 (predicted)	BI296566	3.0
Vascular endothelial growth factor-D (*VEGF-D*)	**AY032728**	**3.0**
Similar to SUMO/sentrin specific protease 5	BE110674	3.0
Mitogen activated protein kinase kinase 1 (*MAP2K1*)	**D13341**	**3.0**
Similar to RIKEN cDNA 0610007P06	AA891221	3.0
Protein phosphatase 1, regulatory subunit 3C (predicted)	**AW530361**	**3.0**

Table 6. Genes upregulated in MNC under hypoxia (>threefold)

Gene name	GenBank accession no.	Fold change
BCL2/adenovirus E1B 19 kDa-interacting protein 3 (*BNIP3*)	NM_053420	34.7
EGL nine homolog 3 (*EGLN3*)	NM_019371	20.6
Similar to low density lipoprotein receptor-related protein binding protein	BI291430	18.8
Arginase 1 (*ARG1*)	NM_017134	13.0
Procollagen-proline, 2-oxoglutarate 4-dioxygenase, α1 polypeptide (*P4HA1*)	BI274401	10.9
Adrenomedullin (*AM*)	NM_012715	10.9
Flavin-containing monooxygenase 5 (*FMO5*)	AI454611	8.3
Enolase 2 (*ENO2*)	AF019973	8.2
Procollagen lysine, 2-oxoglutarate 5-dioxygenase 2 (*PLOD2*)	BI279641	7.9
Pyruvate dehydrogenase kinase 1 (*PDK1*)	NM_053826	7.8
Nidogen 2 (predicted)	BM389302	6.5
Osteopontin (*OSP*)	AB001382	6.5
Macrophage migration inhibitory factor (*MIF*)	NM_031051	6.4
Triosephosphate isomerase 1 (*TPI1*)	NM_022922	6.3
DNA-damage-inducible transcript 4 (*DDIT4*)	NM_080906	6.1
Deleted in liver cancer 1 (*DLC1*)	AI176713	5.9
Solute carrier family 2, member 1 (*SLC2A1*)	BI284218	5.8
Coagulation factor XIII, A1 subunit (*F13A*)	BM388525	5.7
Chemokine (C-X-C motif) ligand 2 (*CXCL2*)	NM_053647	5.5
Aldolase C (*ALDOC*)	NM_012497	5.5
Phosphofructokinase (*PFK1*)	NM_013190	5.4
Adenylate kinase 3-like 1 (*AK3L1*)	AA891949	4.7
Zinc finger protein 503 (predicted)	BF560938	4.7
Phosphoglycerate kinase 1 (*PGK1*)	NM_053291	4.4
ERO1-like (*ERO1L*)	AY071924	4.3
G protein-coupled receptor 128 (predicted)	BM388427	4.3
Very low density lipoprotein receptor (*VLDLR*)	AA849857	4.0
Similar to hypothetical protein FLJ10986	AA926048	4.0
Vascular endothelial growth factor A (*VEGF-A*)	AI175732	3.7
Strongly similar to NP_076005.1 hypoxia-inducible protein 2	BI282296	3.6
Moderately similar to XP_484547.1 (predicted)	AW434319	3.5
ADP-ribosyltransferase 2b (*ART2B*)	AI411747	3.5
Similar to RIKEN cDNA 2010001M09 (predicted)	AI069938	3.4
Histone 2a (*H2A*)	AW533007	3.4
Down syndrome critical region gene 1-like 1 (*DSCR1L1*)	BI274408	3.3
Peripheral myelin protein 22 (*PMP22*)	AA943163	3.3
Monocarboxylate transporter 3 (*MCT3*)	NM_030834	3.3
Moderately similar to NP_080634.1 ovary-specific acidic protein	AA957929	3.3
Strongly similar to XP_128979.3 (predicted)	BG377830	3.2
N-myc downstream regulated gene 1 (predicted)	BE120446	3.2
Transforming growth factor, β-induced (*TGFBI*)	BG379319	3.2
UDP-Gal:βGlcNAc β1,3-galactosyltransferase, polypeptide 3 (predicted)	AA799400	3.2
A kinase (PRKA) anchor protein 7 (*AKAP7*)	BI300893	3.2
Hypothetical gene supported by NM_175764 (*JMJD1A*)	AI172079	3.2
Zinc finger protein 503 (predicted)	AA956230	3.2
Interleukin 1α (*IL1A*)	NM017019	3.1
TCDD-inducible poly(ADP-ribose) polymerase (predicted)	AI511405	3.1
EGL nine homolog 1 (*EGLN1*)	BI282122	3.1
Agrin (*AGRIN*)	BE096523	3.0

Abbreviation: MNC, mononuclear cells.

lung fibroblasts [21, 22]. In the present study, a significant number of exclusively upregulated genes were involved in glycolysis and metabolism; however, this might cause the difference in flexibility between MSC and MNC in response to hypoxia. In fact, focusing on genes encoding secretory proteins, the genes upregulated in MSC under hypoxia, but not in MNC, included several growth factors, such as VEGF-D, PGF, PBEF1, and HB-EGF. VEGF-D has angiogenic properties, and its promoter activity has been shown to increase under hypoxic conditions [23, 24]. Moreover, VEGF-D expression is significantly upregulated in response to hypoxia in differentiating embryonic stem cells [25]. PGF, another member of the VEGF family, is transcriptionally activated by hypoxia [26]. PBEF1 was originally identified as a growth factor for early-stage B cells [27] and has been demonstrated to be upregulated by hypoxia in adipocytes and breast cancer cells [28, 29]. HB-EGF, an EGF family member glycoprotein [30], has been implicated in angiogenesis [31, 32] and enhances the proliferation of MSC via interaction with its receptor, HER-1 [33]. HB-EGF expression has been induced in response to hypoxia in cerebral cortical cultures [34]. Interestingly, the present study demonstrated that MSC upregulated the expression of MMP-9 in response to hypoxia. MMP-9 is a member of metalloproteases [35] and is required for angiogenesis associated with bone growth and revascularization of ischemic tissues [36, 37]. MMP-9 releases soluble Kit-ligand from membrane Kit-ligand, causing the release of stromal-derived factor-1 and the recruitment of $CXCR4^+VEGFR1^+$ hematopoietic progenitors, "hemangiocytes" [38, 39]. These findings, concurrently with our observations, support that MSC act to promote cell proliferation, including angiogenesis, and cell survival in response to hypoxia.

On the other hand, CXCL2 (macrophage inflammatory protein-2) and IL-1α were upregulated in MNC, but not in MSC, under hypoxia. Previous reports demonstrated that *CXCL2* gene expression is strongly induced in macrophages in response to hypoxia [40], and IL-1α production is also induced in peripheral blood MNC under hypoxia [41]. However, in contrast to MSC, no growth factors were specifically upregulated in MNC under hypoxia. It has been suggested that monocyte recruitment, as a consequence of an inflammatory response, is important for promoting angiogenesis via paracrine release of cytokines [42, 43]. Moreover, recent studies have suggested that transplantation of MNC, like that of MSC, induces therapeutic angiogenesis mostly through paracrine effects in ischemic disease [7, 44, 45]. Our observations suggest that transplantation of MNC, unlike that of MSC, may induce an inflammatory response under hypoxia, which may induce angiogenesis.

In the present study, we demonstrated that the gene responses to hypoxia at different time courses and different oxygen concentrations were cell-type-specific. In MSC, seven of the eight genes were upregulated even at 10% O_2 but responded slowly to hypoxia. On the contrary, three of the five enriched genes in MNC responded rapidly to hypoxia but did not reach a peak up to 1% O_2. It remains to be elucidated whether these differences contribute differently to paracrine actions of each type of cells in in vivo situations. Moreover, because bone marrow-derived MNC consists of mixed cell types, such as monocytes, lymphocytes, and erythroblasts, additional studies are needed to clarify which cell types in MNC are responsible for those gene expressions.

Taken together, the difference in gene expression profiles under normoxia and hypoxia, difference in gene expression at various times, and O_2 level between MSC and MNC could cause their distinctive paracrine effects in terms of cell proliferation, including angiogenesis, and cell survival.

SUMMARY

Bone marrow-derived MSC highly expressed a number of genes involved in development and morphogenesis compared with bone marrow-derived MNC. MSC and MNC responded to hypoxia mostly in an exclusive manner; this response might cause the difference in paracrine effects between MSC and MNC in ischemic conditions.

ACKNOWLEDGMENTS

This work was supported by a research Grant for Cardiovascular Disease (16C-6) and Human Genome Tissue Engineering 009 from the Ministry of Health, Labor and Welfare of Japan.

DISCLOSURE OF POTENTIAL CONFLICTS OF INTEREST

The authors indicate no potential conflicts of interest.

REFERENCES

1 Pittenger MF, Martin BJ. Mesenchymal stem cells and their potential as cardiac therapeutics. Circ Res 2004;95:9–20.
2 Minguell JJ, Erices A, Conget P. Mesenchymal stem cells. Exp Biol Med (Maywood) 2001;226:507–520.
3 Tateishi-Yuyama E, Matsubara H, Murohara T et al. Therapeutic angiogenesis for patients with limb ischaemia by autologous transplantation of bone-marrow cells: A pilot study and a randomised controlled trial. Lancet 2002;360:427–435.
4 Tse HF, Kwong YL, Chan JK et al. Angiogenesis in ischaemic myocardium by intramyocardial autologous bone marrow mononuclear cell implantation. Lancet 2003;361:47–49.
5 Perin EC, Dohmann HF, Borojevic R et al. Transendocardial, autologous bone marrow cell transplantation for severe, chronic ischemic heart failure. Circulation 2003;107:2294–2302.
6 Fernández-Aviles F, San Roman JA, Garcia-Frade J et al. Experimental and clinical regenerative capability of human bone marrow cells after myocardial infarction. Circ Res 2004;95:742–748.
7 Kinnaird T, Stabile E, Burnett MS et al. Bone-marrow-derived cells for enhancing collateral development: Mechanisms, animal data, and initial clinical experiences. Circ Res 2004;95:354–363.
8 Hattori R, Matsubara H. Therapeutic angiogenesis for severe ischemic heart diseases by autologous bone marrow cells transplantation. Mol Cell Biochem 2004;264:151–155.
9 Iwase T, Nagaya N, Fujii T et al. Comparison of angiogenic potency between mesenchymal stem cells and mononuclear cells in a rat model of hindlimb ischemia. Cardiovasc Res 2005;66:543–551.
10 Nagaya N, Kangawa K, Itoh T et al. Transplantation of mesenchymal stem cells improves cardiac function in a rat model of dilated cardiomyopathy. Circulation 2005;112:1128–1135.
11 Kinnaird T, Stabile E, Burnett MS et al. Local delivery of marrow-derived stromal cells augments collateral perfusion through paracrine mechanisms. Circulation 2004;109:1543–1549.
12 Kinnaird T, Stabile E, Burnett MS et al. Marrow-derived stromal cells express genes encoding a broad spectrum of arteriogenic cytokines and promote in vitro and in vivo arteriogenesis through paracrine mechanisms. Circ Res 2004;94:678–685.
13 Wakitani S, Saito T, Caplan AI. Myogenic cells derived from rat bone marrow mesenchymal stem cells exposed to 5-azacytidine. Muscle Nerve 1995;18:1417–1426.
14 Silva WA Jr, Covas DT, Panepucci RA et al. The profile of gene expression of human marrow mesenchymal stem cells. STEM CELLS 2003;21:661–669.
15 Jeong JA, Hong SH, Gang EJ et al. Differential gene expression profiling of human umbilical cord blood-derived mesenchymal stem cells by DNA microarray. STEM CELLS 2005;23:584–593.
16 Wagner W, Wein F, Seckinger A et al. Comparative characteristics of mesenchymal stem cells from human bone marrow, adipose tissue, and umbilical cord blood. Exp Hematol 2005;33:1402–1416.
17 Brendel C, Kuklick L, Hartmann O et al. Distinct gene expression profile of human mesenchymal stem cells in comparison to skin fibroblasts employing cDNA microarray analysis of 9600 genes. Gene Expr 2005; 12:245–257.
18 Gnecchi M, He H, Liang OD et al. Paracrine action accounts for marked protection of ischemic heart by Akt-modified mesenchymal stem cells. Nat Med 2005;11:367–368.
19 Gnecchi M, He H, Noiseux N et al. Evidence supporting paracrine hypothesis for Akt-modified mesenchymal stem cell-mediated cardiac protection and functional improvement. FASEB J 2006;20:661–669.
20 Martin-Rendon E, Hale SJ, Ryan D et al. Transcriptional profiling of human cord blood CD133+ and cultured bone marrow mesenchymal stem cells in response to hypoxia. STEM CELLS 2007;25:XX–XX.
21 Bacher M, Schrader J, Thompson N et al. Up-regulation of macrophage migration inhibitory factor gene and protein expression in glial tumor cells during hypoxic and hypoglycemic stress indicates a critical role for angiogenesis in glioblastoma multiforme. Am J Pathol 2003;162:11–17.
22 Baugh JA, Gantier M, Li L et al. Dual regulation of macrophage migration inhibitory factor (MIF) expression in hypoxia by CREB and HIF-1. Biochem Biophys Res Commun 2006;347:895–903.
23 Jussila L, Alitalo K. Vascular growth factors and lymphangiogenesis. Physiol Rev 2002;82:673–700.
24 Teng X, Li D, Johns RA. Hypoxia up-regulates mouse vascular endothelial growth factor D promoter activity in rat pulmonary microvascular smooth-muscle cells. Chest 2002;121(suppl 3):82S–83S.
25 Nilsson I, Rolny C, Wu Y et al. Vascular endothelial growth factor receptor-3 in hypoxia-induced vascular development. FASEB J 2004;18: 1507–1515.
26 Green CJ, Lichtlen P, Huynh NT et al. Placenta growth factor gene expression is induced by hypoxia in fibroblasts: A central role for metal transcription factor-1. Cancer Res 2001;61:2696–2703.
27 Samal B, Sun Y, Stearns G et al. Cloning and characterization of the cDNA encoding a novel human pre-B-cell colony-enhancing factor. Mol Cell Biol 1994;14:1431–1437.
28 Segawa K, Fukuhara A, Hosogai N et al. Visfatin in adipocytes is

upregulated by hypoxia through HIF1alpha-dependent mechanism. Biochem Biophys Res Commun 2006;349:875–882.
29 Bae SK, Kim SR, Kim JG et al. Hypoxic induction of human visfatin gene is directly mediated by hypoxia-inducible factor-1. FEBS Lett 2006;580:4105–4113.
30 Higashiyama S, Abraham JA, Miller J et al. A heparin-binding growth factor secreted by macrophage-like cells that is related to EGF. Science 1991;251:936–939.
31 Abramovitch R, Neeman M, Reich R et al. Intercellular communication between vascular smooth muscle and endothelial cells mediated by heparin-binding epidermal growth factor-like growth factor and vascular endothelial growth factor. FEBS Lett 1998;425:441–447.
32 Arkonac BM, Foster LC, Sibinga NE et al. Vascular endothelial growth factor induces heparin-binding epidermal growth factor-like growth factor in vascular endothelial cells. J Biol Chem 1998;273:4400–4405.
33 Krampera M, Pasini A, Rigo A et al. HB-EGF/HER-1 signaling in bone marrow mesenchymal stem cells: Inducing cell expansion and reversibly preventing multilineage differentiation. Blood 2005;106:59–66.
34 Jin K, Mao XO, Sun Y et al. Heparin-binding epidermal growth factor-like growth factor: Hypoxia-inducible expression in vitro and stimulation of neurogenesis in vitro and in vivo. J Neurosci 2002;22:5365–5373.
35 Chang C, Werb Z. The many faces of metalloproteases: Cell growth, invasion, angiogenesis and metastasis. Trends Cell Biol 2001;11:S37–43.
36 Vu TH, Shipley JM, Bergers G et al. MMP-9/gelatinase B is a key regulator of growth plate angiogenesis and apoptosis of hypertrophic chondrocytes. Cell 1998;93:411–422.
37 Johnson C, Sung HJ, Lessner SM et al. Matrix metalloproteinase-9 is required for adequate angiogenic revascularization of ischemic tissues: Potential role in capillary branching. Circ Res 2004;94:262–268.
38 Heissig B, Hattori K, Dias S et al. Recruitment of stem and progenitor cells from the bone marrow niche requires MMP-9 mediated release of kit-ligand. Cell 2002;109:625–637.
39 Jin DK, Shido K, Kopp HG et al. Cytokine-mediated deployment of SDF-1 induces revascularization through recruitment of CXCR4(+) hemangiocytes. Nat Med 2006;12:557–567.
40 Zampetaki A, Mitsialis SA, Pfeilschifter J et al. Hypoxia induces macrophage inflammatory protein-2 (MIP-2) gene expression in murine macrophages via NF-kappaB: The prominent role of p42/ p44 and PI3 kinase pathways. FASEB J 2004;18:1090–1092.
41 Ghezzi P, Dinarello CA, Bianchi M et al. Hypoxia increases production of interleukin-1 and tumor necrosis factor by human mononuclear cells. Cytokine 1991;3:189–194.
42 Arras M, Ito WD, Scholz D et al. Monocyte activation in angiogenesis and collateral growth in the rabbit hindlimb. J Clin Invest 1998;101:40–50.
43 Sunderkötter C, Steinbrink K, Goebeler M et al. Macrophages and angiogenesis. J Leukoc Biol 1994;55:410–422.
44 Balsam LB, Wagers AJ, Christensen JL et al. Haematopoietic stem cells adopt mature haematopoietic fates in ischaemic myocardium. Nature 2004;428:668–673.
45 Murry CE, Soonpaa MH, Reinecke H et al. Haematopoietic stem cells do not transdifferentiate into cardiac myocytes in myocardial infarcts. Nature 2004;428:664–668.

Available online at www.sciencedirect.com
ScienceDirect
Journal of Molecular and Cellular Cardiology 42 (2007) 88–97
Journal of Molecular and Cellular Cardiology
www.elsevier.com/locate/yjmcc

Original article

Transplantation of mesenchymal stem cells attenuates myocardial injury and dysfunction in a rat model of acute myocarditis

Shunsuke Ohnishi [a,*,1], Bobby Yanagawa [a,1], Koichi Tanaka [a], Yoshinori Miyahara [a], Hiroaki Obata [a,b], Masaharu Kataoka [a], Makoto Kodama [b], Hatsue Ishibashi-Ueda [c], Kenji Kangawa [d], Soichiro Kitamura [e], Noritoshi Nagaya [a,*]

[a] *Department of Regenerative Medicine and Tissue Engineering, National Cardiovascular Center Research Institute, Fujishirodai 5-7-1, Osaka 565-8565, Japan*
[b] *Division of Cardiology, Niigata University Graduate School of Medical and Dental Sciences, Niigata, Japan*
[c] *Department of Pathology, National Cardiovascular Center, Osaka, Japan*
[d] *Department of Biochemistry, National Cardiovascular Center Research Institute, Osaka, Japan*
[e] *Department of Cardiovascular Surgery, National Cardiovascular Center, Osaka, Japan*

Received 11 May 2006; received in revised form 29 August 2006; accepted 2 October 2006
Available online 13 November 2006

Abstract

Acute myocarditis is a non-ischemic inflammatory disease of the myocardium for which there is currently no specific treatment. We have previously shown that mesenchymal stem cells (MSC) can ameliorate heart injury during acute ischemia and in dilated cardiomyopathy; however, the therapeutic potential in acute myocarditis is unclear. In this study, we investigated the ability of MSC to attenuate myocardial injury and dysfunction during the acute phase of experimental myocarditis. Ten-week-old male Lewis rats were injected with porcine myosin to induce myocarditis. Cultured MSC (3×10^6 cells/rat) were injected intravenously 7 days after myosin injection. At 3 weeks, myosin injection resulted in severe inflammation and significant deterioration of cardiac function. MSC transplantation attenuated increases in CD68-positive inflammatory cells and monocyte chemoattractant protein-1 (MCP-1) expression in myocardium, and improved cardiac function in this model. Furthermore, myocardial capillary density was higher in myocarditis tissue, and was further increased by MSC transplantation. *In vitro*, cultured adult rat cardiomyocytes were injured in response to MCP-1, whereas this effect was attenuated by MSC-derived conditioned medium, suggesting cardioprotective effects of MSC acting in a paracrine manner. MSC transplantation attenuated myocardial injury and dysfunction in a rat model of acute myocarditis, at least in part through paracrine effects of MSC.

Keywords: Acute myocarditis; Mesenchymal stem cell; Paracrine effect; Cytokine; Cell death

1. Introduction

Acute myocarditis is a non-ischemic heart disease characterized by myocardial inflammation and edema. This disease is associated with rapidly progressive heart failure, arrhythmias and sudden death [1,2]. Although the early evidence for efficacy of immunoglobulin and interferon therapy appears promising, these results have yet to be demonstrated in randomized or controlled clinical trials. The current options are restricted to supportive care for heart failure or arrhythmias. The lack of specific treatment and the potential severity of the illness emphasize the importance of novel and effective therapeutic strategies for myocarditis.

Mesenchymal stem cells (MSC) are multipotent stem cells present in adult tissues, and have the ability to differentiate into a variety of lineages, including vascular smooth muscle cells, endothelial cells and cardiomyocytes [3,4]. We have previously reported that bone marrow-derived MSC engrafted in experimental myocardial infarction expressed both cardiac and endothelial phenotypes in the heart, and further increased capillary density and decreased the infarct size [5]. Moreover, we have recently demonstrated that monolayered MSC derived from adipose tissue reversed wall thinning in the scar area and improved cardiac function in rats with myocardial infarction [6]. The cardioprotective effects of MSC are known to be mediated

* Corresponding authors. Tel.: +81 6 6833 5012; fax: +81 6 6833 9865.
E-mail addresses: sonsihi@ri.ncvc.go.jp (S. Ohnishi), nnagaya@ri.ncvc.go.jp (N. Nagaya).
[1] Drs Ohnishi and Yanagawa contributed equally to this study.

0022-2828/$ - see front matter © 2006 Elsevier Inc. All rights reserved.
doi:10.1016/j.yjmcc.2006.10.003

not only by their differentiation into vascular cells and cardiomyocytes, but also by their ability to supply large amounts of angiogenic, anti-apoptotic and mitogenic factors [5–7]. These findings suggest the therapeutic potential of MSC for heart failure. However, whether intravenously transplanted MSC attenuate myocardial inflammation and cardiac dysfunction in acute myocarditis remains unknown.

In the present study, we used porcine myosin-induced acute myocarditis in Lewis rats. This model closely resembles human giant cell myocarditis, a frequently fatal disorder characterized by multinucleated giant cells in the myocardium [8]. To examine the therapeutic potential of MSC in the acute phase of myocarditis, MSC were intravenously injected into rats 7 days after myosin injection.

Thus, the purposes of this study were 1) to investigate whether intravenous transplantation of MSC improves cardiac function and pathological findings including myocardial inflammation in rats with myosin-induced myocarditis, and 2) to investigate the underlying mechanisms responsible for the effects of MSC.

2. Materials and methods

2.1. Animals

Ten-week-old male Lewis rats (Japan SLC, Hamamatsu, Japan) were used in all experiments, and were maintained in our animal facilities. The experimental protocols were approved by The Animal Care Committee of the National Cardiovascular Center.

2.2. Preparation of cardiac myosin

Purified cardiac myosin from the ventricular muscle of pig hearts was prepared according to a procedure described previously [8]. The antigen was dissolved at a concentration of 20 mg/ml in phosphate-buffered saline (PBS) containing 0.3 M KCl, mixed with an equal volume of complete Freund's adjuvant containing 11 mg/ml *Mycobacterium tuberculosis* (Difco Laboratories, Sparks, MD, USA). Rats were anesthetized with an intraperitoneal injection of 20 mg/kg sodium pentobarbital, and 0.1 ml of the antigen-adjuvant emulsion was injected into the each footpad.

2.3. Acute myocarditis model

Forty-five rats were randomly divided into three groups and received the following treatment: 1) 0.2 ml saline and sham surgery (Sham group, $n=15$), 2) 0.2 ml cardiac myosin antigen and sham surgery (MyoC group, $n=15$), and 3) 0.2 ml cardiac myosin followed by MSC transplantation 7 days post-myosin injection (MyoC+MSC group, $n=15$). Rats were weighed and observed daily for signs of morbidity and for death.

2.4. Preparation and transplantation of bone marrow-derived MSC

MSC were prepared as described previously [5]. Briefly, bone marrow cells were isolated by flushing out the femoral and tibial cavities with PBS, and plated onto 10-cm dishes in complete culture medium: Dulbecco's Modified Eagle's Medium (DMEM), 15% fetal bovine serum, 100 U/ml penicillin and 100 μg/ml streptomycin. Five days after plating, non-adherent cells were removed, and adherent cells were further propagated for 4 to 5 passages.

Seven days after myosin injection, MSC (3×10^6 cells) or vehicle (0.9% saline) was intravenously administered via the jugular vein. Sham rats also received saline administration but without myosin injection.

2.5. Hemodynamic studies

Hemodynamic studies were performed on day 21 post-myosin injection. Anesthesia was maintained with an intraperitoneal injection of 20 mg/kg sodium pentobarbital, and a 1.5 Fr micromanometer-tipped catheter was placed in the left ventricle through the right carotid artery (Millar Instruments, Houston, TX, USA). Heart rate (HR) was also monitored by electrocardiography. HR, mean arterial pressure (MAP), left ventricular systolic pressure (LVSP), left ventricular end-diastolic pressure (LVEDP), maximum dP/dt (Max dP/dt) and minimum dP/dt (Min dP/dt) were used as indices of hemodynamics, and recorded simultaneously during ventilation after a minimum equilibration period of 20 min.

2.6. Echocardiographic studies

Echocardiography was performed on day 21 post-myosin injection. Rats were anesthetized with an intraperitoneal injection of 20 mg/kg sodium pentobarbital. A 12 MHz probe was placed at the left 4th intercostal space for M-mode imaging using 2D echocardiography (Sonos 5500, Philips, Bothell, WA, USA). Left ventricular systolic dimension (LVDs), left ventricular diastolic dimension (LVDd), anterior wall thickness (AWT), posterior wall thickness (PWT) and ejection fraction (EF) were measured, and taken as an average of three beats. Fractional shortening (%FS) was calculated as $(LVDd-LVDs)/LVDd\times100$.

2.7. Histological examination

The heart was excised above the origin of the great vessels, and heart weight and body weight were recorded on day 21 post-myosin injection. Portions of the midventricular heart, spleen, pancreas, kidney and liver were fixed with 4% paraformaldehyde, embedded in paraffin, sectioned at 4-μm thickness, stained with either hematoxylin and eosin (H & E) or Masson's trichrome, and subjected to immunohistochemical staining. H & E-stained sections were evaluated by a cardiovascular pathologist (H.I.-U.) for the characterization of myocardial injury and inflammation without knowledge of the experimental groups, on the following scale: 0, absent or questionable presence; 1, limited focal distribution; 2–3, intermediate severity; and 4, coalescent and extensive foci throughout the entire transversely sectioned ventricular tissue.

2.8. Immunohistochemical study

Paraffin-embedded heart sections were washed in increasing concentrations of ethanol and then with PBS. Sections were incubated with Protein Block (DakoCytomation, Glostrup, Denmark), then with mouse anti-rat von Willebrand Factor (vWF) (DakoCytomation), CD68 (DakoCytomation) or monocyte chemoattractant protein-1 (MCP-1) (BD Biosciences Pharmingen, San Jose, CA, USA) antibody in diluent for 40 min, followed by incubation with horseradish peroxidase (HRP)-linked rabbit anti-mouse IgG (DakoCytomation) for 30 min. Sections were visualized using 0.5% diaminobenzidine and 0.03% hydrogen peroxide, and counterstained with hematoxylin. The numbers of CD68-stained cells and vWF-stained capillaries were determined in 10 randomly selected fields (×200).

2.9. Enzyme-linked immunosorbent assay (ELISA)

Serum MCP-1 level of rats on day 21 post-myosin injection was measured using a Rat MCP-1 ELISA kit (Biosource International, Carmarillo, CA, USA). Vascular endothelial growth factor (VEGF) and hepatocyte growth factor (HGF) levels in the supernatant of MSC culture (2.3×10^5 cells in 10-cm dish cultured for 48 h) were measured using ELISA kits, according to the manufacturers' protocols (HGF, Institute of Immunology, Tokyo, Japan; VEGF, R&D Systems, Minneapolis, MN, USA).

2.10. Isolation of cardiomyocytes

Ventricular cardiomyocytes were obtained as described previously with modification [9]. Briefly, after heparinization by intraperitoneal injection of 1000 U/kg heparin sodium, the heart was rapidly excised, and pulmonary, connective and other noncardiac tissues were removed. The heart was then mounted on the cannula of a modified Langendorff apparatus and perfused with buffer containing 0.75 mg/ml collagenase type I (Worthington, Lakewood, NJ, USA), 0.5 mg/ml hyaluronidase (Sigma) and 1% bovine serum albumin (fraction V, ICN, Aurora, OH, USA), in a recirculating fashion for 3 h. After the perfusion sequence, the heart was removed from the perfusion apparatus, the atrium was removed, and gently minced. The enzyme-containing buffer was harvested and the cardiomyocytes resuspended in fresh buffer. The calcium concentration in the suspension was raised stepwise to 1.2 mM. Quiescent, calcium-tolerant cardiomyocytes were gravitationally separated from any nonventricular cells and resuspended in complete culture medium. The culture medium was exchanged for fresh medium to remove the damaged myocytes that failed to attach 3 h after plating. After this procedure, 80% to 90% myocytes were viable and showed rod-shape.

2.11. Cardiomyocyte stimulation and MTS assay

To assess cardioprotective effects of MSC acting in a paracrine manner, we investigated whether conditioned medium obtained from MSC culture attenuated MCP-1-induced cardiomyocyte injury. Cardiomyocytes were plated on 96-well plates (1×10^3 viable cells/well) precoated with laminin (BD Biosciences Pharmingen). After 3 h, the medium was changed to fresh DMEM containing 15% FBS or conditioned medium obtained from MSC culture, with or without 50 ng/ml MCP-1 (R&D Systems, Minneapolis, MN, USA). After 24 h, the cellular level of 3-(4,5-dimethylthiazol-2-yl)-5-(3-carboxymethoxyphenyl)-2-(4-sulfophenyl)-2H-tetrazolium (MTS), indicative of the mitochondrial function in living cells and cell viability, was measured ($n=6$) with a CellTiter96 AQueous One Kit (Promega, Madison, WI, USA) and a Microplate Reader (490 nm, Bio-Rad, Hercules, CA, USA).

2.12. In vitro apoptosis assay

Terminal dUTP nick end labeling (TUNEL) assay (ApopTag Fluorescein In Situ Apoptosis Detection Kit, Chemicon International, Temecula, CA, USA) was performed to evaluate apoptosis of cultured cardiomyocytes. After incubation for 24 h, cardiomyocytes were fixed in 1% paraformaldehyde, and TUNEL staining was performed for detection of apoptotic nuclei according to the manufacturer's

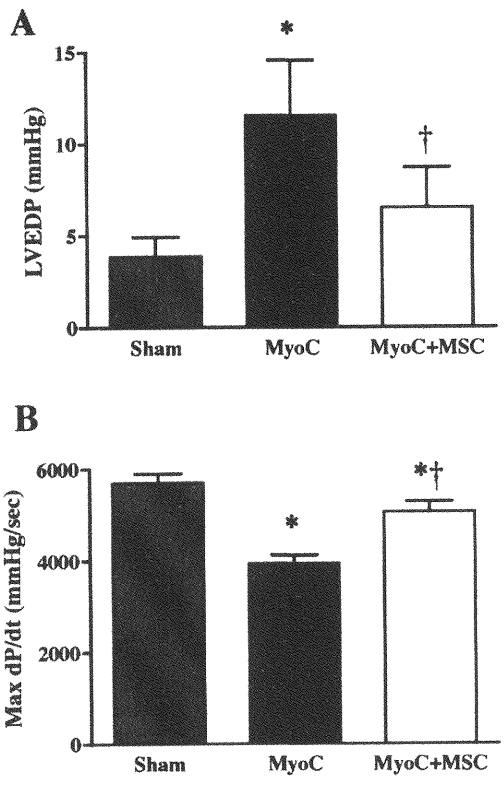

Fig. 1. Effects of MSC transplantation on hemodynamic parameters in acute myocarditis. (A) Left ventricular end-diastolic pressure (LVEDP) and (B) maximum dP/dt (Max dP/dt) were measured in sham-operated rats given vehicle (Sham group), myosin-treated rats given vehicle (MyoC group), and myosin-treated rats given MSC (MyoC+MSC group). Values are mean±S.E. *$P<0.05$ *vs* Sham, †$P<0.05$ *vs* MyoC group.

Table 1
Physiological parameters in three experimental groups

	Sham	MyoC	MyoC+MSC
HW/BW (g/kg)	2.9±0.3	6.4±0.3*	4.7±0.3*,†
HR (bpm)	446±11	363±14*	442±12*,†
MAP (mm Hg)	108±3	87±3*	108±4†
LVSP (mm Hg)	130±2	105±4*	125±4†
Min d*P*/d*t* (mm Hg/s)	−5440±199	−3097±183*	−4617±171*,†

Sham, sham-operated rats given vehicle; MyoC, myosin-treated rats given vehicle; MyoC+MSC, myosin-treated rats given MSC (3×10^6 cells); HW/BW, heart weight to body weight ratio; HR, heart rate; MAP, mean arterial pressure; LVSP, left ventricular systolic pressure; Mim d*P*/d*t*, minimum d*P*/d*t*. Data are mean±S.E. *$P<0.05$ *vs* Sham, †$P<0.05$ *vs* MyoC group.

instructions. The cells were then mounted in medium containing DAPI. Randomly selected microscopic fields ($n=5$) were evaluated to calculate the ratio of TUNEL-positive cells to total cells.

Table 2
Echocardiographic findings in three experimental groups

	Sham	MyoC	MyoC+MSC
LVDs (mm)	3.1±0.1	5.0±0.4*	3.8±0.2†
EF (%)	74.9±1.2	56.6±3.4*	71.2±3.5†
AWT diastole (mm)	1.9±0.1	3.0±0.2*	3.0±0.3*
PWT diastole (mm)	1.9±0.1	3.4±0.1*	2.7±0.2*,†

Sham, sham-operated rats given vehicle; MyoC, myosin-treated rats given vehicle; MyoC+MSC, myosin-treated rats given MSC (3×10^6 cells); LVDs, left ventricular systolic dimension; EF, ejection fraction; AWT, anterior wall thickness; PWT, posterior wall thickness. Data are mean±S.E. *$P<0.05$ *vs* Sham, †$P<0.05$ *vs* MyoC group.

2.13. Creatine kinase (CK) activity assay

CK activity in culture media was measured after incubation of cardiomyocytes for 24 h ($n=5$), using the enzyme measurement kit (Kanto Chemical, Tokyo, Japan).

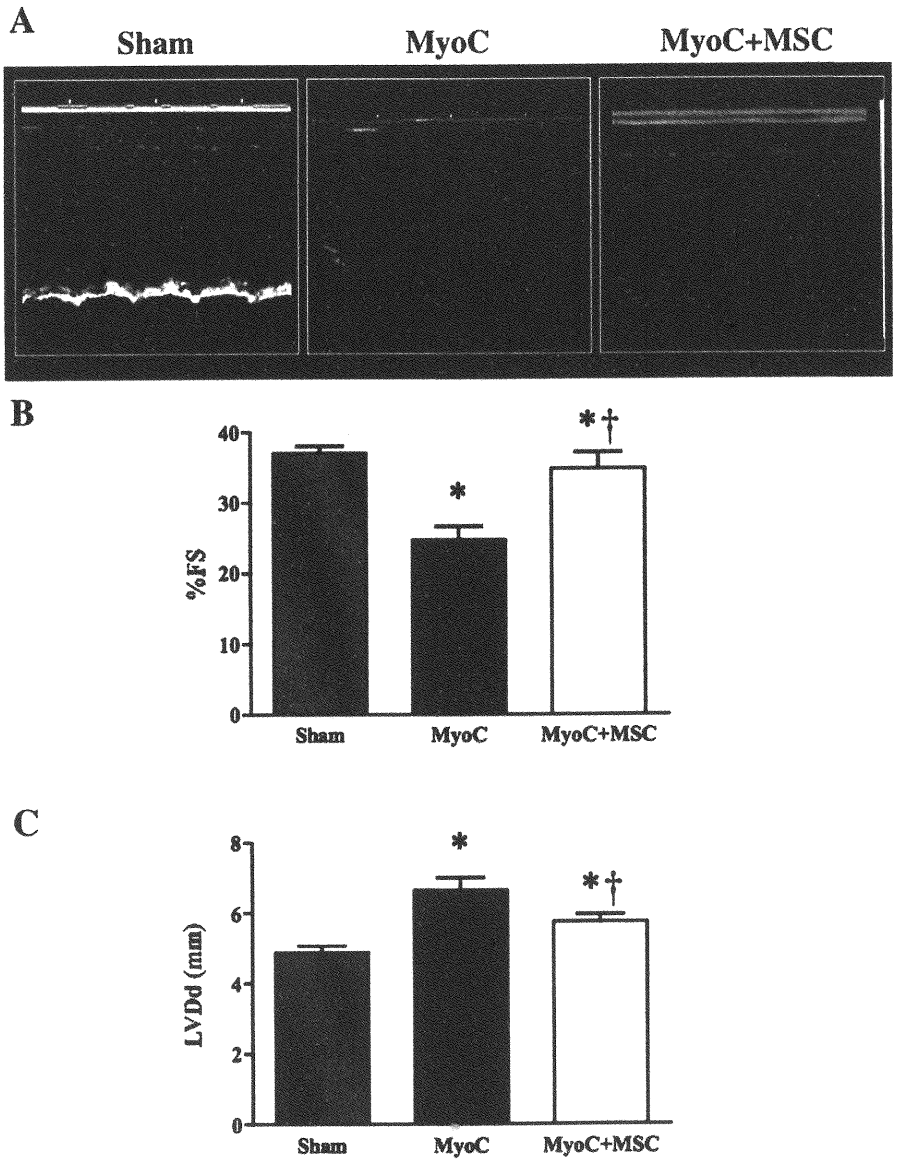

Fig. 2. Effects of MSC transplantation on echocardiographic parameters in acute myocarditis. (A) Representative echocardiographic images showing wall thickening and poor movement in the MyoC group, and improvement of cardiac contractility in the MyoC+MSC group. (B and C) MSC transplantation significantly improved fractional shortening (%FS) and left ventricular diastolic dimension (LVDd). Values are mean±S.E. *$P<0.05$ *vs* Sham, †$P<0.05$ *vs* MyoC group.